# Conformational Study of the Macrocycle 1,4,7-Trithiacyclononane in Metal Complexes†

**Joanne Beech,**[a,b] **Peter J. Cragg**[a] **and Michael G. B. Drew** *[,a]
[a] *Department of Chemistry, The University, Whiteknights, Reading RG6 2AD, UK*
[b] *AWE plc, Aldermaston, Reading RG7 4PR, UK*

---

Computational studies have been carried out on the macrocycle 1,4,7-trithiacyclononane [9]ane$S_3$ in the free state and in metal complexes. A range of metal complexes of [9]ane$S_3$ has been studied by molecular mechanics and good agreement has been obtained with experimental structural data. The macrocycle forms a series of octahedral complexes M([9]ane$S_3$)$_2$, with M–S bond lengths ranging between 2.241 Å for $Fe^{II}$ to 2.725 Å for $Ag^{I}$. Changes in the geometry of the macrocycle upon binding to different metals in these complexes have been successfully modelled. Also studied were a range of less-symmetric structures containing this macrocycle and the reasons for the wide variations in conformation have been established.

---

Molecular mechanics has been used for many years to study the structures and properties of organic molecules[1] and the results are usually as accurate as can be obtained experimentally. Many attempts have been made to expand its capability to include inorganic systems.[2-6] However, there are significant difficulties involved in the parametrisation of those parts of the structure involving the metals which have not yet been overcome. It has proved possible to obtain good parameters for a range of similar systems by systematic fitting to X-ray data. A good example of this approach is provided by Adam *et al.*[4] who studied 18 macrocyclic complexes of $Ni^{2+}$ and obtained good transferable parameters for nickel. However this process took a great deal of time and only provided one set of metal parameters which could be used with a particular set of macrocycles. It is clearly desirable to derive methods that can provide parameters easily for a complete set of elements and ways of doing this have recently been suggested by Rappe *et al.*[7] with their universal force field (UFF). In this work each atom in the Periodic Table is described by a set of hybridisation-dependent atomic bond radii, a set of hybridisation angles, van der Waals parameters, torsional and inversion barriers and a set of effective nuclear charges. For a particular molecule the force-field parameters for bonds, angles, torsion angles, and non-bonded interactions are then generated from these atomic properties.

In previous work we have used our in-house version of the MM2 program which has been suitably adapted[8] to cater for metal systems. We have worked in a similar fashion to Adam *et al.*,[4] and obtained parameters for metals by careful parametrisation so that we could investigate their macrocyclic complexes.[9,10] We were interested in the possibility of being able to derive parameters for a whole range of metals quickly and easily using the UFF procedure and therefore decided to evaluate the procedure. We searched for a macrocycle which formed complexes with a wide range of metals and for which much structural data was available and chose 1,4,7-trithianonane ([9]ane$S_3$). Polysulfur macrocycles act as chelating ligands for an extensive range of metals[11] and of these [9]ane$S_3$ is by far the most studied with well over 30 crystal structures having been determined to date. Many of these have the stoichiometry M([9]ane$S_3$)$_2$ with the metal bonded to six equidistant sulfur atoms in an octahedral environment. In addition there are distorted structures of this stoichiometry as well as complexes containing just one [9]ane$S_3$ together with other ligands.

The main part of this paper describes the modelling of these metal complexes. However we also carried out a search on the possible conformations of [9]ane$S_3$ in the free state and this is described first.

## Conformational Analysis of [9]ane$S_3$

The crystal structure of the free macrocycle has been determined and shows an *endo* conformation with crystallographically imposed $C_3$ symmetry.[12] Independent torsion angles are successively S–C–C–S −58.6, C–C–S–C 131.1, and C–S–C–C −55.0°. This conformation is found in many complexes as the three sulfur atoms are available for facial co-ordination to metal ions. The macrocycle has also been studied by electron diffraction in the gas phase.[13] The data were incompatible with this conformation but two others were considered possible, with $C_2$ and $C_1$ symmetry (see later).

Conformational search procedures for cyclic systems have been much discussed recently[14-18] and a variety of methods have been recommended. The determination of the global minimum and all local minima is not trivial even for a relatively small ring system like [9]ane$S_3$. We used three different methods, molecular dynamics, random search and grid scan from the Quanta/CHARMm package.[19] The [9]ane$S_3$ molecule was built up on the Quanta/CHARMm package. For molecular mechanics minimisation, default parameters in the force field were used as were template atomic charges. All structures were first minimised with steepest descents for 1000 cycles and then conjugate gradients until convergence when the gradient was less than 0.000 01 kcal $mol^{-1}$ $Å^{-1}$.

(*a*) *Molecular Dynamics*.—The molecule was subjected to a molecular dynamics calculation. The step size was 1 fs and the temperature was 2000 K. One thousand conformations of the molecule were saved at 1 ps intervals and were later refined by molecular mechanics.

(*b*) *Grid Scan*.—A C–C bond was set up as an elastic bond. During the grid scan this bond is considered to be 'broken' and the molecule as acyclic with $CH_2$ groups at the two ends. There are now six torsion angles along the backbone of the molecule and these were selected for the grid scan and given three possible values of 60, −60 and 180° so that $3^6 = 729$ conformations were studied. When each trial conformation of the molecule had been constructed, then the elastic bond was reformed and the structure minimised by molecular mechanics. Frequencies were scaled up to a total of 1000 for comparison with the molecular dynamics data.

---

† *Non-SI unit employed:* cal = 4.184 J.

(*c*) *Random Search*.—As in the grid-scan method, a C–C bond was set up as an elastic bond and the six torsion angles along the backbone were selected. Each angle was allowed to change randomly by up to 50° and the resulting structure was then saved. We then used this subsequent structure for further random changes and repeated the procedure to obtain 1000 different conformations which were saved and later minimised by molecular mechanics.

## Results and Discussion

*Conformational Search Methods*.—All three methods located 13 different conformations of [9]ane$S_3$ with an energy range of 4.53–8.52 kcal $mol^{-1}$. These are listed as (a)–(m) inclusive in Table 1 and their torsion angles are in Table 2. In addition there were a few sightings of five other conformations with energy in excess of 17.4 kcal $mol^{-1}$ [(n)–(r) inclusive in Table 1] but the population of these would be zero for all but the highest temperatures so they are not included in our subsequent analysis. All three methods have located the same 13 lowest-energy conformations and the frequencies are comparable if not equivalent. It seems most unlikely that any conformations have been missed and we believe the analysis to be complete.

These conformations were initially distinguished by their final molecular mechanics energy. However we also compared the structural differences between the various conformations by calculating the root mean square (r.m.s.) deviation between atomic positions using the method of Dollase.[20] Since the ring contains three equivalent $SCH_2CH_2$ moieties this is not a straightforward process. For each pair of conformations, twelve fits were attempted automatically using the MATCH program.[21] Hydrogen atoms were omitted and atoms 1–9 in the first structure were first fitted to atoms 1–9 inclusive in the second structure. Then the atoms in the second structure were changed by one or more of the following operations: permutation by 3 or 6, changing the sign of the *x* co-ordinates and reversing the order of atoms (*i.e.* atoms 1–9 reordering to atoms 9–1). The minimum value of the r.m.s. fit for each pair of conformers is reproduced in Table 3. The minimum fit between conformers is 0.41 Å which shows that all 13 conformers are indeed independent and represent different structures.

We also attempted molecular mechanics minimisation using the Newton–Raphson procedure and found that conformers (l) and (m) were unstable and both reverted to (b). This feature of minimisation should perhaps be emphasised as it is not always recognised that different minimisation routines (as well as different force fields) can lead to different minima. Indeed when we used the CERIUS package[22] on these conformers, using the UFF force field, four of the thirteen conformers, *viz.* (c), (k), (l) and (m), were unstable to the Fletcher–Powell minimisation and reverted to (b), (i), (b) and (b) respectively.

**Table 1** Frequencies of observations of the various conformations of [9]ane$S_3$ using different search procedures

| | Frequency | | | |
|---|---|---|---|---|
| Conformation | Molecular dynamics | Grid search | Random search | Energy/ kcal $mol^{-1}$ |
| (a) | 48 | 11 | 55 | 4.53 |
| (b) | 204 | 132 | 166 | 4.84 |
| (c) | 178 | 49 | 76 | 5.39 |
| (d) | 8 | 13 | 7 | 5.99 |
| (e) | 58 | 89 | 158 | 7.57 |
| (f) | 74 | 185 | 172 | 7.53 |
| (g) | 124 | 133 | 38 | 5.13 |
| (h) | 57 | 40 | 82 | 8.13 |
| (i) | 49 | 64 | 36 | 7.47 |
| (j) | 22 | 35 | 45 | 7.31 |
| (k) | 34 | 105 | 30 | 8.52 |
| (l) | 93 | 41 | 95 | 6.78 |
| (m) | 48 | 47 | 20 | 8.27 |
| (n) | 1 | 21 | 11 | 17.45 |
| (o) | — | 5 | 4 | 18.12 |
| (p) | 2 | 21 | 4 | 20.67 |
| (q) | — | 8 | — | 29.67 |
| (r) | — | 1 | 1 | 66.12 |

*Comparison with Experimental Data*.—As discussed above the crystal structure of [9]ane$S_3$ shows the macrocycle in conformation (a). In their work on interpreting the electron diffraction pattern of [9]ane$S_3$, Blom *et al.*[13] only considered conformations (a), (b), (d) and (g). They concluded that (b) and (g) can both be fitted satisfactorily to the experimental data. They did not rule out the possibility that both conformers are present in a mixture, but noted that (b) gives both the lowest *R* factor in the electron diffraction analysis and the lowest strain energy in MM2 calculations and concluded that it is highly probable that this conformer is the major constituent of gaseous [9]ane$S_3$ at about 500 K. As shown in the following section, conformation (a) is by far the most common in the solid state, though (b), (e) and (g) are observed in a few cases.

*Modelling of Metal Complexes*.—Over 30 metal complexes of [9]ane$S_3$ have been characterised by X-ray crystallography and these can be separated into four distinct types: (*i*) octahedral $[M([9]aneS_3)_2]^{n+}$ complexes (Table 4), (*ii*) complexes containing one [9]ane$S_3$ in conformation (a), (Table 5), (*iii*) square-planar complexes of $[M([9]aneS_3)_2]^{n+}$ (Table 6) and (*iv*) other complexes (Table 7).

The most common type is the $[M([9]aneS_3)_2]^{n+}$ octahedral complex in which both ligands have conformation (a) with all sulfur atoms equidistant from the metal (Fig. 1). Despite the plethora of low-energy conformations for the ligand in the gas phase, all the octahedral $[M([9]aneS_3)_2]^{n+}$ compounds show

**Table 2** Different conformations of [9]ane$S_3$ characterised by the torsion angles listed successively around the ring starting at a S–C–C–S angle

| | | Torsion angles/° | | | | | | | | |
|---|---|---|---|---|---|---|---|---|---|---|
| Conformation | Energy/kcal $mol^{-1}$ | | | | | | | | | |
| (a) | 4.53 | −48.2 | 137.6 | −67.0 | −48.2 | 137.6 | −67.0 | −48.2 | 137.6 | −67.0 |
| (b) | 4.84 | −96.0 | 68.2 | −123.5 | 64.9 | 76.8 | −121.3 | 75.0 | −89.2 | 141.8 |
| (c) | 5.39 | −118.2 | 138.1 | −89.3 | 62.0 | −92.6 | 161.8 | −52.6 | −52.1 | 96.1 |
| (d) | 5.99 | −141.8 | 61.3 | 61.3 | −141.8 | 61.3 | 61.3 | −141.8 | 61.3 | 61.3 |
| (e) | 7.57 | −48.0 | −68.2 | 86.9 | 36.9 | −143.9 | 61.3 | 38.0 | −117.3 | 137.4 |
| (f) | 7.53 | −127.5 | 97.8 | −104.4 | 44.6 | 86.3 | −76.5 | −68.2 | 72.5 | 59.0 |
| (g) | 5.13 | −70.5 | −61.0 | 111.3 | −89.4 | 111.3 | −61.0 | −70.5 | 74.8 | 74.8 |
| (h) | 8.13 | 110.7 | −46.8 | −57.9 | 166.3 | −101.8 | 54.6 | −94.7 | 129.6 | −120.5 |
| (i) | 7.47 | −68.7 | −61.5 | 147.1 | −39.0 | −44.9 | −114.7 | −147.3 | 57.9 | 60.7 |
| (j) | 7.31 | 137.9 | −68.5 | −68.5 | 137.9 | −84.5 | 92.6 | −136.1 | 92.6 | −84.5 |
| (k) | 8.52 | −151.9 | 52.7 | 37.4 | −110.0 | 145.1 | −60.6 | −56.2 | 75.6 | 58.2 |
| (l) | 6.78 | 90.1 | −53.6 | 97.8 | −141.1 | 108.5 | −102.1 | 47.1 | 68.3 | −160.4 |
| (m) | 8.27 | −150.2 | 96.8 | −66.9 | 84.3 | −143.0 | 137.1 | −32.1 | −45.9 | 126.8 |

**Table 3** Root mean square deviations (Å) in atomic positions calculated for the 13 conformations of [9]ane$S_3$. Hydrogen atoms are excluded

| | (a) | (b) | (c) | (d) | (e) | (f) | (g) | (h) | (i) | (j) | (k) | (l) | (m) |
|---|---|---|---|---|---|---|---|---|---|---|---|---|---|
| (a) | — | 0.65 | 0.76 | 0.74 | 0.45 | 0.68 | 0.87 | 0.80 | 0.63 | 0.81 | 0.70 | 0.68 | 0.68 |
| (b) | | — | 0.49 | 0.76 | 0.63 | 0.58 | 0.46 | 0.64 | 0.69 | 0.76 | 0.60 | 0.51 | 0.59 |
| (c) | | | — | 0.85 | 0.65 | 0.77 | 0.61 | 0.70 | 0.63 | 0.83 | 0.71 | 0.69 | 0.42 |
| (d) | | | | — | 0.86 | 0.80 | 0.78 | 0.62 | 0.69 | 0.57 | 0.59 | 0.79 | 0.77 |
| (e) | | | | | — | 0.50 | 0.76 | 0.70 | 0.74 | 0.72 | 0.77 | 0.65 | 0.67 |
| (f) | | | | | | — | 0.61 | 0.65 | 0.44 | 0.63 | 0.63 | 0.48 | 0.69 |
| (g) | | | | | | | — | 0.81 | 0.72 | 0.76 | 0.53 | 0.74 | 0.78 |
| (h) | | | | | | | | — | 0.70 | 0.46 | 0.53 | 0.62 | 0.53 |
| (i) | | | | | | | | | — | 0.72 | 0.54 | 0.50 | 0.51 |
| (j) | | | | | | | | | | — | 0.70 | 0.64 | 0.73 |
| (k) | | | | | | | | | | | — | 0.67 | 0.65 |
| (l) | | | | | | | | | | | | — | 0.41 |
| (m) | | | | | | | | | | | | | — |

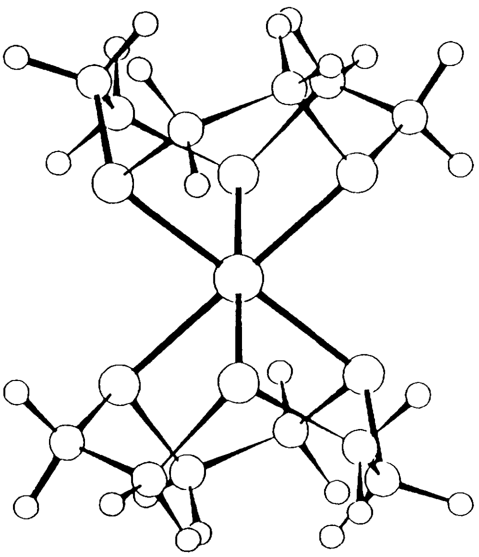

**Fig. 1** Crystal structure of $[Co([9]aneS_3)_2]^{2+}$, showing the (a,a) conformation

both macrocycles in conformation (a). Most of the other conformations (Fig. 2) do not contain the three sulfur atoms in a potentially facial arrangement. However one other suitable conformation of the macrocycle is (e) and so we built two alternative octahedral $[M([9]aneS_3)_2]^{n+}$ structures, one with both macrocycles in conformation (e) and the other with one macrocycle in (a) and the second in (e). The energies of these three conformers (a,a), (a,e) and (e,e) were than calculated as a function of the M–S bond length in the following manner. The M–S bond lengths were fixed at a particular value by giving these bonds a large force constant of 3000 kcal mol$^{-1}$ Å$^{-2}$. The structure was then minimised with this constraint. The effect of this calculation is that the two macrocycles by necessity adjust their conformations to fit in with the enforced M–S bond length[8,9] and the energy is an indication of the resulting strain in the macrocycles. This calculation was then repeated over a range of bond lengths at 0.05 Å intervals from 1.90 to 3.20 Å and the results are shown in Fig. 3. Hancock *et al.*[23] plotted the strain energies of the (a,a) $[M([9]aneS_3)_2]^{n+}$ cations as a function of the covalent radius of the metal ion and found that the lowest energy (corresponding to the best fit) is for a M–S distance of 2.31 Å. We calculated the energy of the minima for the (a,a), (a,e) and (e,e) structures at similar values, *viz.* 2.27, 2.28, and 2.29 Å respectively. The curve for the (a,e) structure almost bisects the (a,a) and (e,e) curves and it is therefore not included in Fig. 3.

The (a,a) structure is lower in energy than the (e,e) structure by *ca.* 5 kcal mol$^{-1}$ over the whole range of M–S bond lengths, thus clearly demonstrating why this conformation is found with such a wide range of metal sizes. The exess of energy for the (a,e) and (e,e) structures is predominantly found in angle-bending terms around the metal atom, although torsion-angle and van der Waals terms are also higher. Even so in the (a,a) conformer the macrocycle does undergo some conformational strain even with the minimum-energy bond length of 2.27 Å and has an energy of 11.96 compared to 8.89 kcal mol$^{-1}$ in the free state.* This strain is caused by the necessity to decrease the S$\cdots$S distances to form the complex. Thus the S$\cdots$S distances are 3.20 Å in the metal complex compared to 3.41 Å in the ideal conformation.

For these calculations we used the default values in the universal force field,[7] with Fe$^{II}$ as the metal, provided by the CERIUS software package with just one exception. It was necessary to change the ideal angle at sulfur for M–S–C and C–S–C angles from 92.2 to 98.0°. This latter value is the default value in CHARMm and it proved to be more appropriate for our calculations.

In the crystal structures of octahedral $[M([9]aneS_3)_2]^{n+}$ complexes variations in S–M–S bond angles and in torsion angles within the ring are observed and these can be correlated with the M–S bond length (Table 4). Thus as the M–S bond length increases [*e.g.* from 2.241 Å (M = Fe$^{II}$) to 2.725 Å (M = Ag$^{I}$)] the S–M–S bond angle becomes smaller (from 89.7 to 79.1°) and the torsion angles change (S–C–C–S increases from −43.9 to −60.7, C–C–S–C changes from 133.1 to 128.1 and from −69.4 to −51.8°). Complexes with intermediate M–S distances for the most part have bond and torsion angles intermediate between the two extremes.

In Fig. 4 we show variations in S–M–S bond angles and S–C–C–S, C–S–C–C and C–C–S–C torsion angles with the ideal bond lengths as calculated using the (a,a) conformation. Also included are points representing the experimental data from all the octahedral crystal structures in Table 4. While structures do vary slightly from the values calculated particularly for the longer bond lengths, the plot indicates a good fit to the experimental data. We conclude that this technique of fixing the M–S bond length, while allowing the rest of the structure to minimise, does give a good indication of the effect of metal co-ordination upon the conformation of the ligand.

*Parametrisation of the force field.* However our primary aim was to find a set of parameters to model all the complexes

---

* All energies in the first part of the paper concerned with conformational analysis were calculated using CHARMm. Those in the second part concerned with metal complexes were calculated using CERIUS. The energies cannot be compared quantitatively. For this calculation therefore we compare the energies of the macrocycle using CERIUS [where the minimum energy of conformation (a) is 8.89 kcal mol$^{-1}$] rather than CHARMm (4.52 kcal mol$^{-1}$).

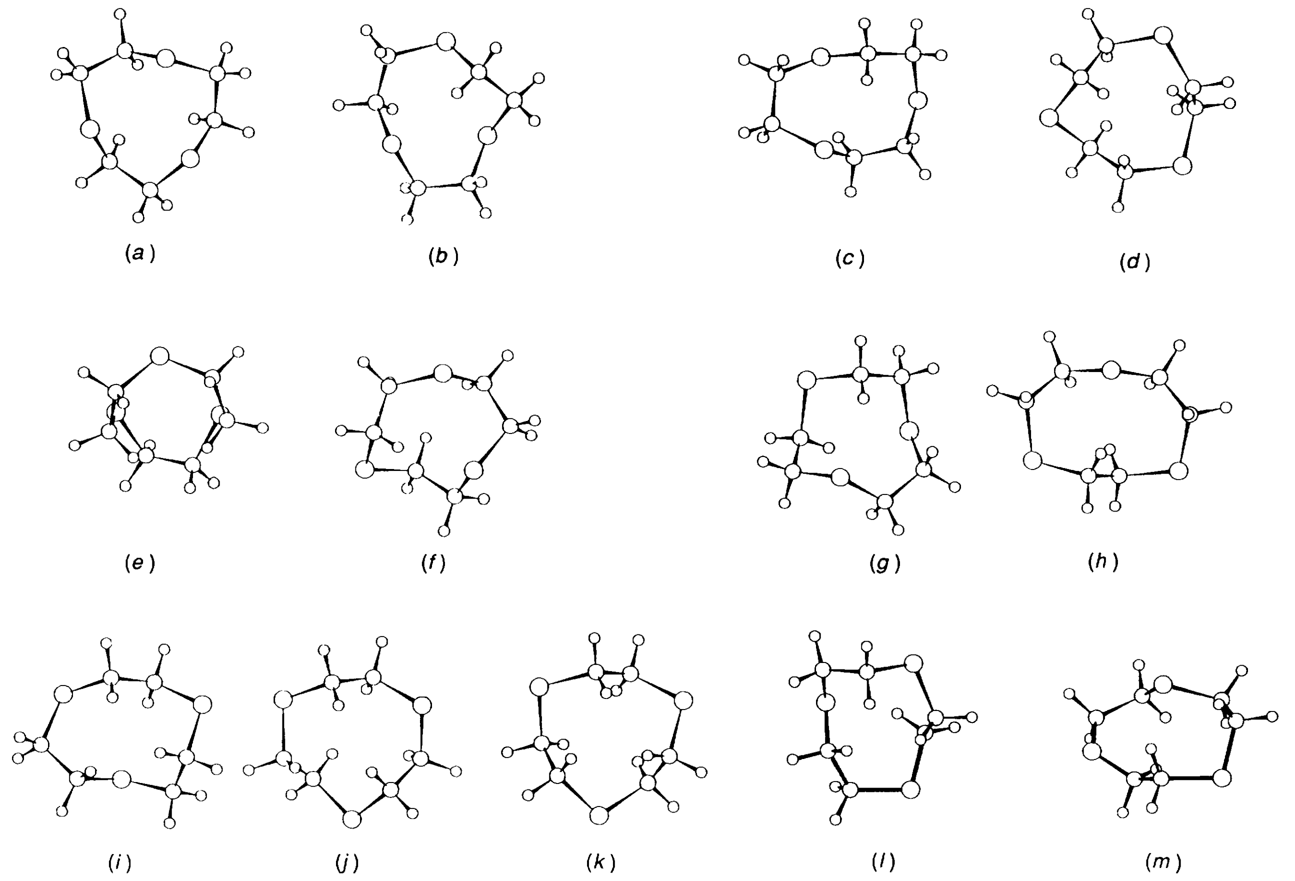

**Fig. 2** The 13 low-energy conformations of [9]ane$S_3$ in the gas phase

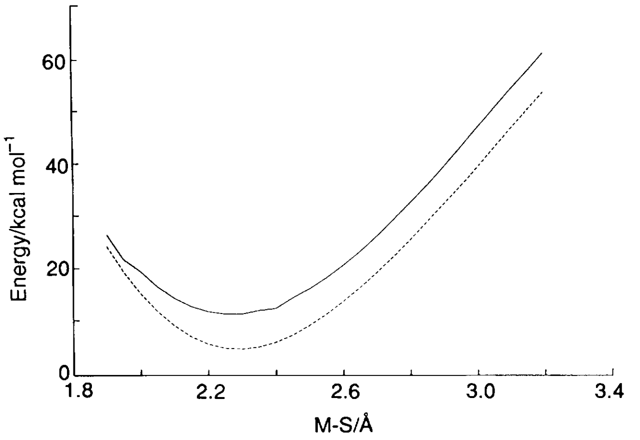

**Fig. 3** Variation in steric energy *vs.* M–S bond length for octahedral $[M([9]aneS_3)_2]^{n+}$ complexes in the (a,a), (– – –) and (e,e), (——) conformations

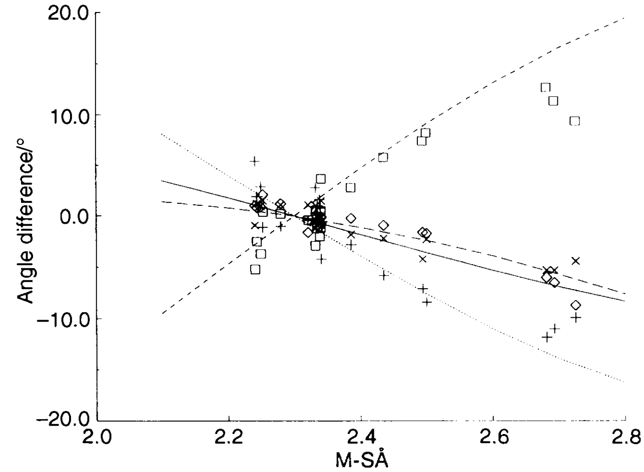

**Fig. 4** Variations in S–M–S bond angles (— — —) and torsion angles S–C–C–S (· · · ·), C–C–S–C (——) and C–S–C–C (- - - -) *vs.* M–S bond length for octahedral $[M([9]aneS_3)_2]^{n+}$ complexes. All angles are referenced to values obtained at an ideal bond length of 2.30 Å, *viz.* S–M–S 88.7, S–C–C–S −49.3, C–C–S–C 134.0, C–S–C–C −64.2° which are taken as 0.0°. Values found in crystal structures are added [S–M–S (◇), S–C–C–S (+), C–C–S–C (×), C–S–C–C (□)]

directly. We first attempted to model the experimental structures directly with the UFF. This force field[7] provides parameters for all elements based on a range of properties such as atomic radii, ideal angles, and effective nuclear charges. Ideal bond lengths are generated from the atomic radii ($r_i$, $r_j$ for atoms *i,j*) plus a bond-order correction, plus an electronegativity correction [eqn. (1)] and all bond-length force

$$r_{ij} = r_i + r_j + r_{BO} + r_{EN} \qquad (1)$$

constants were calculated from equation (2) where $Z^*_i, Z^*_j$

$$k_{ij} = 664.12\, Z^*_i Z^*_j / r_{ij} \qquad (2)$$

are the effective nuclear charges of atoms *i* and *j* and $r_{ij}$ is the ideal bond length. Most workers find that the value of the ideal metal–donor atom bond length is the most important parameter in the force field for inorganic complexes.

In the version of CERIUS used in our work neither the bond order nor electronegativity corrections were implemented.

**Table 4** Dimensions in the crystal structures of the type $[M([9]aneS_3)_2]^{n+}$ with symmetrical $MS_6$ octahedral co-ordination spheres. Codenames in the Cambridge Crystallographic Database are given. Structures with deviations of more than 0.05 Å in M–S distances are included but marked with an asterisk

| | | | | Mean torsion angles/° | | |
|---|---|---|---|---|---|---|
| Codename | M | Mean M–S distance/Å | Mean S–M–S chelate angle/° | S–C–C–S | C–C–S–C | C–S–C–C |
| FUBJUH* | $Fe^{II}$ | 2.241 | 89.7 | −43.9 | 133.1 | −69.4 |
| FUBKAO | $Fe^{II}$ | 2.244 | 89.5 | −47.4 | 135.2 | −66.7 |
| DIBJED | $Fe^{II}$ | 2.250 | 89.6 | −46.4 | 135.0 | −67.9 |
| DOVBAR | $Co^{III}$ | 2.253 | 90.8 | −50.4 | 135.5 | −63.8 |
| KAWTUX | $Fe^{III}$ | 2.280 | 89.9 | −50.3 | 135.1 | −64.0 |
| BOXMIK* | $Co^{II}$ | 2.321 | 87.1 | −49.7 | 135.1 | −64.6 |
| FESKIX | $Ru^{II}$ | 2.332 | 88.0 | −46.5 | 132.8 | −67.1 |
| FENDUX | $Ru^{II}$ | 2.339 | 87.7 | −47.7 | 134.0 | −66.2 |
| VEXGIO | $Ru^{II}$ | 2.340 | 88.0 | −48.5 | 133.8 | −65.3 |
| KIGPOF | $Ru^{II}$ | 2.335 | 87.8 | −48.3 | 133.9 | −65.4 |
| GEMJUD | $Rh^{III}$ | 2.333 | 88.8 | −49.0 | 135.0 | −63.7 |
| JEKROG | $Ir^{III}$ | 2.340 | 88.6 | −49.9 | 133.5 | −63.7 |
| FOSCOF | $Rh^{III}$ | 2.341 | 88.6 | −53.5 | 135.5 | −60.5 |
| BOXMEG | $Ni^{II}$ | 2.386 | 88.5 | −52.1 | 132.2 | −61.4 |
| BOXMOQ | $Cu^{II}$ | 2.435 | 87.8 | −55.1 | 131.8 | −58.4 |
| VEJNON | $Zn^{II}$ | 2.494 | 87.1 | −56.4 | 129.8 | −56.8 |
| VEXGAG | $Zn^{II}$ | 2.500 | 87.0 | −57.7 | 131.7 | −56.0 |
| VEXGEK | $Hg^{II}$ | 2.681 | 82.7 | −61.1 | 128.7 | −51.5 |
| KIFCAD* | $Hg^{II}$ | 2.693 | 82.2 | −60.3 | 128.7 | −52.8 |
| FIJTOH* | $Ag^{I}$ | 2.725 | 80.0 | −59.2 | 129.6 | −54.8 |

However we do not consider this to be a significant disadvantage as this equation clearly represents an over-simplification when applied to M–X bond lengths which are affected by many structural–electronic effects, not only metal radii and electronegativity but also resonance, metal–ligand π bonding, metal–ligand π-back bonding, the *trans* effect and the general effect of the other ligands in the system.[7] In addition there are significant problems in establishing suitable values for all the parameters used, neither atom radius nor electronegativity can be easily estimated and many different values have been published. We found that most ideal M–S bond lengths generated from the atomic properties in the UFF were unsuitable and therefore decided to obtain the best possible parameters for the metal moiety in the $[9]aneS_3$ structures by fitting to the experimental data and the values used for each element are listed in Table 8.* However we used equation (2) to calculate the force constants for the bonds.

Other parameters in the UFF were used unchanged apart from the following. For atom types H_, C_3 and S_3 + 2, the radii were changed to 0.240, 0.760 and 1.059 Å respectively as default values lead to unreasonable bond lengths. The ideal angle for S_3 + 2 was changed to 98.0°. For complexes which contain bonds between metals and other donor atoms ideal values for these bonds were also selected to fit with observed values. Ideal angles at the metal were restricted to 90 and 180° for octahedral and square-planar geometries and 109.54° for tetrahedral geometry, while the two-co-ordinate species described below were treated individually. The angle-bending term was described with a cosine Fourier-expansion term.

*Octahedral* $[M([9]aneS_3)_2]^{n+}$ *complexes.* The observed and calculated structures for the $[M([9]aneS_3)_2]^{n+}$ octahedral structures are detailed in Table 8(*a*). There is an excellent fit in bond lengths and angles concerning the metal atom and also in the torsion angles in the macrocycle. For all structures the average difference in M–S bond length is less than 0.01 Å. The average difference in S–M–S bond angle is less than 2.0° with just two exceptions (both for M = $Hg^{II}$, 3.1 and 2.6°) and the average deviation in torsion angles is less than 4.0°.

$[M([18]aneS_6)]^{n+}$ *complexes.* As stated above, our ideal M–S bond lengths are not likely to be suitable for M–S bonds in all complexes. However we thought it likely that they would allow us to reproduce structures between metals and different thioalkanes. Accordingly, we tested these parameters on a range of 1,4,7,10,13,16-hexathiacyclooctadecane ($[18]aneS_6$) complexes. Results of molecular mechanics minimisations are in Table 9 and show a similarly good agreement with experimental data. The S–M–S angles and torsion angles in the macrocycles are also well reproduced and so it would seem that our M–S bond parameters are appropriate for thioalkane structures.

*Complexes containing one* $[9]aneS_3$ *in conformation* (*a*). These complexes (Table 5) can be classified into four types. Type (*a*) is octahedral with three facial monodentate ligands {*cf.* $[Re(CO)_3([9]aneS_3)]^+$ [Fig. 5(*a*)] and $[PtMe_3([9]aneS_3)]^+$}. Type (*b*) is tetrahedral with just one donor atom in addition to the macrocycle {as in $[CuI([9]aneS_3])$ [Fig. 5(*b*)], $[AgCl([9]aneS_3)]$, $[Cu_2([9]aneS_3)_3]^{2+}$ [Fig. 5(*c*)] and $[Ag_3([9]aneS_3)_3]^{3+}$ [Fig. 5(*d*)]}. The last two are particularly interesting in that the metal atom is bonded to three sulfur atoms of one ligand and one sulfur atom of another. In $[Cu_2([9]aneS_3)_3]^{2+}$ the Cu-S distance to the tridentate $[9]aneS_3$ ligand is 2.32 Å and to the sulfur of a bridging $[9]aneS_3$ ligand is 2.24 Å. This bridging macrocycle has conformation (g) with all torsion angles differing from ideal values listed in Table 2 by less than 10°. In $[Ag_3([9]aneS_3)_3]^{3+}$ the trimer has a crystallographic three-fold axis and one sulfur atom of the macrocycle bridges two metal atoms. As in the copper complex, the bond length to the unique sulfur is less

---

* An alternative approach would be to establish the ideal value by a survey of crystal structures. We searched the Cambridge Crystallographic Database[24] for M–S bond lengths but for the majority of metals found a wide range of distances, even when the selection was restricted to sulfur bonded to carbon. To take two elements at random, Ni–S bonds varied from 2.05 to 2.75 Å (599 examples) and Ir–S bond lengths from 2.15 to 2.56 Å (66 examples). Of course bond lengths varied with the oxidation state, denticity and co-ordination number, but even restricting the survey to six-co-ordinate complexes of $Ni^{II}$ and $Ir^{III}$ still left a wide range of bond lengths. Our conclusion was that it was extremely difficult (if not impossible) to choose ideal M–S bond lengths from the Cambridge database for a specific metal unless the survey was restricted to compounds related to those under study.

**Table 5** Dimensions in crystal structures of metal complexes containing only one [9]aneS$_3$ macrocycle

| Codename | Compound | Torsion angles/° | | | | | | | | | M–S/Å | Mean S–M–S/° |
|---|---|---|---|---|---|---|---|---|---|---|---|---|
| (*a*) Co-ordination number 6, octahedral geometry | | | | | | | | | | | | |
| FIKSEX | $[PtMe_3([9]aneS_3)]^+$ | −52.9 | 134.8 | −59.6 | −52.9 | 132.8 | −64.4 | −48.8 | 130.8 | −62.4 | 2.41 | 88.0 |
| KAXWAH | $[RhL'([9]aneS_3)]^{2+}$ | −50.2 | 134.4 | −63.7 | −49.7 | 133.1 | −63.6 | −50.4 | 134.0 | −63.9 | 2.32 | 88.9 |
| VAVGII | $[CoL'([9]aneS_3)]^{3+}$ | −45.8 | 132.5 | −68.3 | −44.5 | 132.4 | −66.9 | −49.3 | 137.7 | −68.6 | 2.25 | 90.2 |
| JEMMET | $[ReO_3([9]aneS_3)]^{+a}$ | | | | | | | | | | | |
| JARHEP | $[Mn(CO)_3([9]aneS_3)]^{+a}$ | | | | | | | | | | | |
| CUXGAD | $[Mo(CO)_3([9]aneS_3)]$ | −46.6 | 129.1 | −65.2 | −50.1 | 132.6 | −63.8 | −49.7 | 132.3 | −64.5 | 2.52 | 82.8 |
| GIFLAI | $[Re(CO)_3([9]aneS_3)]^+$ | −49.6 | 132.6 | −63.8 | −49.8 | 131.7 | −63.8 | −49.1 | 131.6 | −62.9 | 2.46 | 84.8 |
| | | −49.6 | 131.1 | −64.3 | −50.3 | 132.4 | −58.4 | −54.3 | 135.0 | −63.6[b] | | |
| KILSAZ | $[SbCl_3([9]aneS_3)]$ | −54.3 | 130.4 | −58.4 | −55.8 | 132.2 | −56.9 | −56.4 | 129.3 | −58.3 | 3.10 | 65.9 |
| (*b*) Co-ordination number 4, tetrahedral geometry | | | | | | | | | | | | |
| JAPXUT | $[Cu_2([9]aneS_3)_3]^{2+}$ | −54.6 | 131.9 | −59.6 | −51.6 | 129.1 | −64.0 | −49.6 | 129.4 | −60.3 | 2.32 | 93.9 |
| | | −50.8 | 129.8 | −61.9 | −51.5 | 130.1 | −59.4 | −52.9 | 131.8 | −62.7[b] | | |
| FITDUH | $[CuI([9]aneS_3)]$ | −52.8 | 130.4 | −57.9 | −54.5 | 130.7 | −61.6 | −50.2 | 129.9 | −62.2 | 2.33 | 93.2 |
| JAVWIM | $[AgCl([9]aneS_3)]$ | −54.9 | 125.7 | −61.4 | −51.5 | 128.0 | −58.0 | −57.9 | 131.2 | −54.3 | 2.61 | 84.4 |
| FITDOB | $[Ag_3([9]aneS_3)_3]^{3+}$ | −47.9 | 126.5 | −65.0 | −50.2 | 126.8 | −56.9 | −57.3 | 131.1 | −60.3 | (2.48–2.75) | |
| (*c*) Co-ordination number 5, distorted geometry | | | | | | | | | | | | |
| KILRUS | $[Rh(C_2H_4)_2([9]aneS_3)]^+$ | −48.8 | 130.0 | −62.8 | −42.4 | 135.2 | −62.6 | −51.7 | 136.2 | −65.1 | 2.38 | 86.3 |
| | | −48.7 | 129.9 | −63.9 | −50.0 | 137.2 | −64.4 | −48.8 | 135.1 | −64.1[b] | | |
| KILRIH | $[Rh(cod)([9]aneS_3)]^+$ | −48.9 | 130.5 | −64.3 | −51.0 | 133.2 | −62.1 | −51.2 | 136.4 | −64.6[c] | 2.39 | 86.6 |
| KILROM | $[Ir(cod)([9]aneS_3)]^+$ | −56.7 | 142.0 | −52.6 | −60.8 | 137.6 | −54.1 | −61.2 | 142.8 | −59.9 | 2.36 | 86.2 |
| (*d*) Other structures | | | | | | | | | | | | |
| JAGNUA | $[Fe(\eta\text{-}C_5H_5)([9]aneS_3)]^+$ | −44.5 | 135.2 | −68.2 | −44.9 | 134.4 | −70.2 | −45.0 | 135.6 | −69.8 | 2.21 | 90.6 |
| SITYAV | $[Tl([9]aneS_3)]^+$ | −56.6 | 130.9 | −54.9 | −56.8 | 129.2 | −58.7 | −53.8 | 128.3 | −57.2 | 3.10 | 67.4 |

[a] Disordered. [b] Torsion angles in the second molecule in the asymmetric unit. Bond lengths and angles are averaged over both molecules. [c] A second molecule in the asymmetric unit is disordered.

**Table 6** Dimensions in crystal structures of square-planar [9]ane$S_3$ complexes. Structures have been divided *via* ligand conformation into three groups

| Codename | M | Torsion angles/° | | | | | | | | | M–S/Å | |
|---|---|---|---|---|---|---|---|---|---|---|---|---|
| | | | | | | | | | | | eq. | ax. |
| (*a*) $[M([9]aneS_3)_2]^{n+}$ with both ligands in conformation (a) | | | | | | | | | | | | |
| FIKRUM | $Pd^{III}$ | −53.7 | 129.5 | −57.8 | −55.1 | 134.7 | −59.5 | −53.8 | 133.2 | −60.6 | 2.355 | 2.545 |
| FAPBAZ | $Pd^{II}$ | −48.6 | 131.3 | −57.9 | −58.4 | 120.8 | −47.4 | −62.1 | 137.8 | −62.5 | 2.324 | 2.952 |
| FAPBED | $Pd^{II}$ | −49.9 | 132.0 | −58.8 | −61.0 | 123.1 | −47.4 | −62.9 | 138.5 | −60.4 | 2.311 | 3.005 |
| KAMXUR | $Au^{III}$ | −64.1 | 127.4 | −48.0 | −61.4 | 135.9 | −57.3 | −55.7 | 132.5 | −54.9 | 2.35 | 2.93 |
| KESDIV | $Au^{II}$ | −51.0 | 124.7 | −59.5 | −55.8 | 130.2 | −53.5 | −59.4 | 133.2 | −59.9 | 2.457 | 2.839 |
| (*b*) $[M([9]aneS_3)_2]^{2+}$ with ligands in conformations (a) and (b) | | | | | | | | | | | | |
| FAGSAH | $Pt^{II}$ | | | | | | | | | | | |
| | Molecule 1 | 32.9 | −117.5 | 67.6 | 45.9 | −131.6 | 65.8 | 56.1 | −119.2 | 66.9 | 2.280 | 2.878 |
| | | −68.1 | 76.7 | −140.7 | 51.4 | 66.8 | −106.2 | 88.9 | −107.0 | 105.4 | | |
| | 2 | 55.7 | −118.5 | 50.3 | 59.3 | −134.5 | 56.8 | 51.8 | −132.7 | 64.1 | 2.280 | 2.923 |
| | | −71.1 | 78.5 | −139.0 | 49.1 | 70.0 | −98.3 | 83.1 | −111.0 | 109.4 | | |
| (*c*) Square-planar $[MX_2([9]aneS_3)]$ with the ligand in conformation (e) | | | | | | | | | | | | |
| FAPBIH | $Pd^{II}$ X = Br | 39.6 | 80.0 | −57.8 | −61.3 | 125.6 | −103.7 | 46.2 | 51.9 | −138.2 | 2.265 | 3.125 |
| GATLES | $Pd^{II}$ X = Cl | 41.9 | 77.8 | −58.4 | −59.6 | 123.4 | −105.1 | 48.2 | 50.1 | −138.7 | 2.257 | 3.140 |

**Table 7** Dimensions in crystal structures of other complexes containing [9]ane$S_3$ with distorted structures

| Codename | Compound | | Torsion angles/° | | | | | | | | |
|---|---|---|---|---|---|---|---|---|---|---|---|
| JEKRIA | $[IrH([9]aneS_3)_2]^{2+}$ | | | | | | | | | | |
| | | (a) | −53.5 | 134.8 | −6.7 | −49.8 | 136.5 | −67.3 | −61.2 | 132.2 | −61.3 |
| | | (b) | −40.0 | −77.5 | 92.6 | −74.4 | 109.1 | −107.2 | 61.9 | −76.9 | 134.5 |
| | | | Ir–S/Å 2.32 (mean equatorial), 2.48 (axial) | | | | | | | | |
| KAMXOL | $[Au([9]aneS_3)_2]^{+}$ [a] | | | | | | | | | | |
| | | (g) | 69.5 | 57.5 | −105.1 | 84.5 | −102.5 | 56.9 | 69.0 | −72.1 | −70.9 |
| | | (e) | −44.9 | 129.1 | −77.4 | −24.3 | 108.1 | −120.6 | 33.5 | 76.6 | −71.7 |
| | | | Au–S/Å 2.346 (× 1), 2.295 (× 1), 2.791 (× 2) | | | | | | | | |
| JAFLEH | *catena*-$[AuCl([9]aneS_3)]$ | | | | | | | | | | |
| | | (g) | −58.4 | −68.3 | 102.1 | −80.9 | 106.7 | −60.3 | −64.7 | 59.3 | 78.9 |
| | | | Au–S/Å 2.270 (× 1) | | | | | | | | |
| VEJNIH | $[Pb(ClO_4)_2([9]aneS_3)_2]$ [b] | | | | | | | | | | |
| | | (a) | 53.2 | −129.7 | 58.1 | 57.2 | −129.3 | 53.5 | 59.7 | −137.8 | 60.6 |
| | | | Pb–S/Å 3.015–3.129 (× 6), Pb-O 2.719 (× 2) | | | | | | | | |

[a] A second molecule in the asymmetric unit is disordered. [b] Eight-co-ordinate, bonded to six sulfurs and two monodentate perchlorate ions.

(2.472 Å) than the bond length to the tridentate ligand (2.724, 2.595, 2.613 Å). There is also an interesting series of five-co-ordinate complexes [type (*c*)] in which the metal is sandwiched between [9]ane$S_3$ and two ethene bonds *e.g.*$[Rh(cod)([9]aneS_3)]^+$ (cod = cycloocta-1,5-diene) [Fig. 5(*e*)]. Finally type (*d*) includes two unique structures $[Fe(\eta\text{-}C_5H_5)([9]aneS_3)]^+$ [Fig. 5(*f*)] where the metal is sandwiched between a cyclopentadienyl ring and the macrocycle and $[Tl([9]aneS_3)]^+$ where the thallium can be described as three-co-ordinate though there are weak interactions with other cations and the $PF_6^-$ anions.

We modelled all these structures and the results are in Table 8(*b*). The results are not as close to experimental data as those from the octahedral $[M([9]aneS_3)_2]^{n+}$ compounds. However the average bond-length deviation for each structure is less than 0.02 Å with the exceptions of $[CuI([9]aneS_3)]^+$ (0.022 Å) and $[Fe(\eta\text{-}C_5H_5)([9]aneS_3)]^+$ (0.038 Å). The average deviation in angle is less than 3° with the exception of $[CoL'([9]aneS_3)]^{3+}$ (L′ = 1,4,7-triazacyclononane) (3.6°) and the average deviation in torsion angle in the macrocycle is less than 4° with the exceptions of $[Mo(CO)_3([9]aneS_3)]$ (6.1), $[CuI([9]aneS_3)]$ (4.0), and $[Ag_3([9]aneS_3)_3]^{3+}$ (4.2°). Average deviations summed over all the structures are 0.01 Å, 1.5° and 2.8° for bonds, angles and torsion angles respectively.

Of the less well modelled compounds both $[CuI([9]aneS_3)]$ and $[Ag_3([9]aneS_3)_3]^{3+}$ contain metal ions that are prone to irregular co-ordination geometries and the silver complex is part of a trinuclear system which is likely to induce strain into individual metal geometries. In the tricarbonyl complexes $[Mo(CO)_3([9]aneS_3)]$ and $[Re(CO)_3([9]aneS_3)]^+$ the ligand conformations are somewhat unexpected for M–S bond lengths of 2.52 (Mo) and 2.46 Å (Re) as the mean torsion angles are *ca.* −49, 134 and −63° instead of the predicted −56, 132 and −57°. These experimental torsion angles are more characteristic of structures with shorter M–S bond lengths. It may be significant that these structures contain π-bonding ligands (carbonyls, cyclopentadienyl) in addition to the [9]ane$S_3$.

*Square-planar complexes* $[M([9]aneS_3)_2]^{n+}$. Apart from the symmetric structures (Table 4), some complexes of $[M([9]aneS_3)_2]^{n+}$, particularly with $d^8$ metal ions, have been reported with square-planar distortions and these are listed in Table 6. Results of minimisation are in Table 8(*c*). These molecules exhibit four short distances in the equatorial plane with significant axial distortion. The conformation of the ligand in these complexes {with the notable exception of $[Pt([9]aneS_3)_2]^{2+}$} is similar to those found in the symmetrical complexes. The extent of the bond-length elongation in the axial direction is dependent upon the metal ranging from

0.19 Å for M = $Pd^{III}$ to 0.69 Å for M = $Pd^{II}$. The irregularity of the torsion angles can be correlated with variations in bond length. For example in $[Pd([9]aneS_3)_2]^{2+}$, FAPBED [Fig. 5(*g*)], the S–C–C–S torsion angle involving the two sulfur atoms strongly bound to the metal in the equatorial plane is −49.9° compared to −61.0 and −62.9° for the other two angles and similar distortions are found in the other axially distorted structures.

The complex $[Pd([9]aneS_3)]^{3+}$ was modelled by assigning six equivalent bonds around the metal and the minimisation produced a regular co-ordination sphere and did not reproduce the small axial distortion. To model the more severely axially distorted complexes we assigned square-planar geometry with non-bonded axial sulfur atoms. Unlike the symmetric $[M([9]aneS_3)_2]^{n+}$ complexes, where it is necessary for the $[9]aneS_3$ macrocycle to adopt a facial conformation, for the asymmetric complexes many different conformations of the macrocycle seem possible. Structures with (b,b), (e,e) and (g,g) conforma-

**Table 8** Comparison of dimensions in molecular mechanics-minimised structures with those from crystal structures (below in italics)

| | M–S/Å | | | Mean S–M–S/° | Mean torsion angles/° | | |
|---|---|---|---|---|---|---|---|
| M | Ideal | Refined | Structures | Refined | S–C–C–S | C–C–S–C | C–S–C–C |
| (*a*) $[M([9]aneS_3)_2]^{n+}$ with symmetrical $MS_6$ octahedral co-ordination spheres (*cf.* Table 4) | | | | | | | |
| $Fe^{II}$ | 2.240 | 2.245 | FUBJUH, FUBKAO, DIBJED | 89.9 | −47.9 | 134.9 | −66.2 |
| | | *2.245* | | *89.6* | *−45.9* | *134.4* | *−68.0* |
| $Fe^{III}$ | 2.279 | 2.280 | KAWTUX | 89.5 | −49.2 | 134.9 | −64.8 |
| | | *2.280* | | *89.9* | *−50.3* | *135.1* | *−64.0* |
| $Co^{II}$ | 2.324 | 2.321 | BOXMIK | 88.9 | −50.7 | 134.2 | −63.1 |
| | | *2.321* | | *87.1* | *−49.7* | *135.1* | *−64.6* |
| $Co^{III}$ | 2.240 | 2.245 | DOVBAR | 89.9 | −47.9 | 135.5 | −66.2 |
| | | *2.253* | | *90.8* | *−50.4* | *135.5* | *−63.8* |
| $Ni^{II}$ | 2.395 | 2.385 | BOXMEG | 88.0 | −52.9 | 133.2 | −60.6 |
| | | *2.386* | | *88.5* | *−52.1* | *132.2* | *−61.4* |
| $Cu^{II}$ | 2.457 | 2.435 | BOXMOQ | 86.7 | −54.0 | 132.6 | −59.3 |
| | | *2.435* | | *87.8* | *−55.1* | *131.8* | *−58.4* |
| $Zn^{II}$ | 2.536 | 2.497 | VEJNON, VEXGAG | 85.1 | −55.3 | 132.0 | −57.8 |
| | | *2.498* | | *86.0* | *−57.0* | *130.7* | *−56.4* |
| $Ru^{II}$ | 2.337 | 2.335 | FESKIX, FENDUX, VEXGIO | 89.2 | −51.6 | 133.9 | −62.0 |
| | | *2.337* | | *87.9* | *−47.6* | *133.5* | *−66.2* |
| $Rh^{III}$ | 2.329 | 2.329 | FOSCOF, GEMJUD | 89.1 | −51.5 | 134.0 | −62.2 |
| | | *2.337* | | *88.7* | *−51.2* | *135.2* | *−62.1* |
| $Ag^{I}$ | 2.762 | 2.725 | FITJOH, FITDOB | 78.4 | −60.0 | 128.9 | −53.3 |
| | | *2.725* | | *79.5* | *−59.2* | *129.6* | *−54.8* |
| $Ir^{III}$ | 2.348 | 2.344 | JEKROG | 89.2 | −52.1 | 133.7 | −61.5 |
| | | *2.340* | | *88.6* | *−49.9* | *133.5* | *−63.7* |
| $Hg^{II}$ | 2.729 | 2.688 | VEXGEK, KIFCAD | 79.6 | −57.8 | 131.0 | −55.1 |
| | | *2.687* | | *82.4* | *−60.7* | *128.7* | *−52.1* |
| (*b*) Structures containing one $[9]aneS_3$ ligand (*cf.* Table 5) | | | | | | | |
| $Pt^{IV}$ | 2.406 | 2.405 | FIKSEX | 87.3 | −53.1 | 133.4 | −60.4 |
| | | *2.406* | | *88.0* | *−51.5* | *132.8* | *−62.1* |
| $Rh^{III}$ | 2.329 | 2.329 | KAXWAH | 88.9 | −50.7 | 134.1 | −63.1 |
| | | *2.328* | | *88.9* | *−50.1* | *133.8* | *−63.7* |
| $Co^{III}$ | 2.240 | 2.263 | VAVGII | 86.6 | −46.4 | 136.6 | −68.1 |
| | | *2.247* | | *90.2* | *−46.5* | *134.2* | *−67.9* |
| $Mo^{0}$ | 2.533 | 2.520 | CUXGAD | 85.2 | −56.3 | 131.6 | −56.6 |
| | | *2.520* | | *82.8* | *−48.8* | *134.6* | *−64.5* |
| $Re^{I}$ | 2.470 | 2.460 | GIFLAI | 86.9 | −55.3 | 132.1 | −57.8 |
| | | *2.460* | | *84.8* | *−50.4* | *132.4* | *−62.8* |
| $Sb^{III}$ | 3.123 | 3.102 | KILSAZ | 65.8 | −58.7 | 138.0 | −57.2 |
| | | *3.102* | | *65.9* | *−57.9* | *130.6* | *−55.5* |
| $Cu^{I\,a}$ | 2.345 | 2.317 | JAPXUT | 96.1 | −56.8 | 131.0 | −56.0 |
| | | *2.322* | | *93.9* | *−51.8* | *130.3* | *−61.3* |
| $Ag^{I\,a}$ | 2.635 | 2.601 | JAVWIM | 83.3 | −54.9 | 130.6 | −57.9 |
| | | *2.605* | | *84.4* | *−54.8* | *128.3* | *−57.9* |
| $Cu^{I\,b}$ | 2.345 | 2.313 | FITDUH | 95.4 | −56.3 | 131.2 | −56.7 |
| | | *2.335* | | *93.2* | *−52.5* | *130.3* | *−60.6* |
| $Ag^{I\,b}$ | 2.635 | 2.609 | FITDOB | 81.5 | −56.2 | 132.4 | −56.8 |
| | | *2.603* | | *82.5* | *−51.8* | *128.1* | *−60.7* |
| $Rh^{I}$ | 2.378 | 2.384 | KILRUS | 85.8 | −49.9 | 134.2 | −63.8 |
| | | *2.378* | | *86.3* | *−48.4* | *133.9* | *−63.8* |
| $Rh^{I}$ | 2.378 | 2.382 | KILRIH | 86.4 | −51.2 | 134.2 | −62.5 |
| | | *2.393* | | *86.6* | *−50.4* | *133.4* | *−63.7* |
| $Ir^{I}$ | 2.378 | 2.359 | KILROM | 86.5 | −50.7 | 134.6 | −63.1 |
| | | *2.360* | | *86.2* | *−55.5* | *140.8* | *−59.6* |
| $Fe^{II}$ | 2.240 | 2.246 | JAGNUA | 93.2 | −51.6 | 134.2 | −62.1 |
| | | *2.208* | | *90.6* | *−44.8* | *135.1* | *−69.4* |
| $Tl^{I\,c}$ | 3.129 | 3.107 | SITYAV | 64.6 | −60.0 | 132.9 | −53.4 |
| | | *3.108* | | *67.4* | *−55.7* | *129.5* | *−56.9* |

**Table 8** (*continued*)

| M | M–S/Å Ideal | M–S/Å Refined | Structures | Mean S–M–S/° Refined | Mean torsion angles/° S–C–C–S | C–C–S–C | C–S–C–C |
|---|---|---|---|---|---|---|---|
| (*c*) Square-planar complexes (*cf.* Table 6) | | | | | | | |
| Pd$^{\mathrm{III}}$ | 2.432 | 2.422 | FIKRUM | 87.6 | −54.4 | 132.6 | −58.9 |
| | | *2.423* | | *87.8* | *−54.2* | *132.5* | *−59.3* |
| Pd$^{\mathrm{II}}$[a] | 2.264 | 2.318, 3.005 | FAPBAZ | 89.9 | −59.2 | 130.1 | −53.2 |
| | | *2.324, 2.952* | | *88.6* | *−55.7* | *130.0* | *−56.4* |
| Pd$^{\mathrm{II}}$[a] | 2.264 | 2.318, 3.004 | FAPBED | 89.9 | −53.2 | 130.1 | −59.2 |
| | | *2.311, 3.005* | | *89.2* | *−55.5* | *131.2* | *−57.9* |
| Pt$^{\mathrm{II}}$[a] | 2.280 | 2.280, 2.863 | FAGSAH | 90.3 | −57.2 | 131.2 | −55.6 |
| | | *2.280, 2.878* | | *89.0* | *−50.3* | *125.7* | *−61.9* |
| Pd$^{\mathrm{II}}$[a] | 2.264 | 2.263, 3.141 | FAPBIH | 90.2 | *d* | | |
| | | *2.265, 3.125* | | *89.7* | | | |
| Pd$^{\mathrm{II}}$[a] | 2.264 | 2.263, 3.134 | GATLES | 90.2 | *d* | | |
| | | *2.257, 3.140* | | *89.7* | | | |
| (*d*) Other complexes (*cf.* Table 7) | | | | | | | |
| Ir$^{\mathrm{III}}$ | 2.348 | 2.346 | JEKRIA | 89.5 | *d* | | |
| | | *2.352* | | *87.9* | | | |
| Au$^{\mathrm{III}}$[a] | 2.358 | 2.352, 2.918 | KAMXUR | 89.0 | −58.2 | 130.5 | −54.4 |
| | | *2.351, 2.926* | | *89.6* | *−60.4* | *131.9* | *−53.4* |
| Au$^{\mathrm{II}}$[a] | 2.470 | 2.457, 2.908 | KESDIV | 82.7 | −53.5 | 130.1 | −59.0 |
| | | *2.457, 2.839* | | *87.7* | *−55.4* | *129.4* | *−57.6* |
| Au$^{\mathrm{I}}$[e,f] | 2.317 | 2.314 | KAMXOL | 143.7 | *d* | | |
| | | *2.315* | | *155.2* | | | |
| Au$^{\mathrm{I}}$[e,g] | 2.271 | 2.270 | JAFLEH | 172.9 | *d* | | |
| | | *2.270* | | *176.3* | | | |

[a] Four-co-ordinate. [b] Refined as a trimer. [c] Three-co-ordinate. [d] Irregular. [e] Two-co-ordinate. [f] Ideal angle 155°. [g] Ideal angle 175°.

**Table 9** Metal–sulfur bond lengths in $[\mathrm{M([18]aneS_6)}]^{n+}$ metal complexes

| Codename | M | M–S/Å Exptl. | Calc. |
|---|---|---|---|
| KIGRAT | Ru$^{\mathrm{II}}$ | 2.331 | 2.339 |
| CEPCEF | Co$^{\mathrm{II}}$ | 2.340 | 2.321 |
| BUXJEJ | Ni$^{\mathrm{II}}$ | 2.387 | 2.382 |
| DOFBAB | Cu$^{\mathrm{II}}$ | 2.454 | 2.409 |
| KAZWUD | Ag$^{\mathrm{I}}$ | 2.743 | 2.674 |

tions were generated and minimised. Results for $[\mathrm{Pd([9]aneS_3)_2}]^{2+}$, which are representative of all four structures, were 13.68 (a,a), 15.18 (b,b), 18.89 (e,e) and 26.56 kcal mol$^{-1}$ (g,g) thus confirming that conformation (a,a) has the lowest energy for the asymmetric as well as the symmetric structures. The energy of the asymmetric (a,a) complex at 13.68 kcal mol$^{-1}$ is far higher than that found for the symmetric complex with the same ideal bond length (5.26 kcal mol$^{-1}$) thus indicating that the symmetric arrangement is much less strained. The observed asymmetry in the torsion angles in the ring is also reproduced with the S–C–C–S torsion angles −49.6 (unique) and −63.7, −63.4° compared to the experimental values of −49.9, −61.0 and −62.9°. All these structures with axial distortions were accurately reproduced with average deviations of 0.005° in M–S bond length, 0.04 Å in M···S non-bonded distance, 1.9° in S–M–S angle and 1.6° in torsion angle.

The structure of $[\mathrm{Pt([9]aneS_3)_2}]^{2+}$ [Fig. 5(*h*)] is unique in that one macrocycle has conformation (a) and the other (b). The metal is four-co-ordinate with a square-planar environment (Pt–S 2.28 Å). In the ligand with conformation (a) the third sulfur atom is bent towards the metal at a distance of 2.90 Å. However in the ligand with conformation (b) the sulfur is bent away from the metal at 4.04 Å thus producing a distorted square-pyramidal five-co-ordinate environment. Using this structure as a starting model we built the conformations (a,a), (a,b) and (b,b). Respective energies were 10.90 (a,a), 12.64 (a,b) and 14.25 kcal mol$^{-1}$ (b,b). The reasons why $[\mathrm{Pt([9]aneS_3)_2}]^{2+}$ has the (a,b) structure are unclear. There are two molecules in the asymmetric unit both with the same conformation and we were unable to find any significant packing effects that might cause this conformation to occur. However the difference between the structures (a,a) and (a,b) is only 1.74 kcal mol$^{-1}$. The minimisation of the structure did reproduce all torsion angles in conformation (b) of the macrocycle to within 7° and described well the significant variations from that gas-phase conformation. The macrocycle with conformation (b), despite considerable variations in torsion angles, is not very strained with an energy of 11.97 kcal mol$^{-1}$ compared to an ideal value of 9.41 kcal mol$^{-1}$.

Also included in Table 6 are two four-co-ordinate complexes *e.g.* $[\mathrm{PdBr_2([9]aneS_3)}]$ [Fig. 5(*i*)] with the metal in a square-planar conformation. The equatorial plane contains two halide ions and two strongly bound sulfur atoms with the axial position occupied by the third sulfur atom at a much longer distance (*e.g.* 3.13 Å). Here the macrocycle has conformation (e) (all angles within 15° of the ideal values in Table 2) different from the (a) observed in the symmetrical $[\mathrm{M([9]aneS_3)_2}]^{2+}$ complexes in Table 4. In our modelled structure the torsion angles are comparable to within 15° of experimental values. The energy of the macrocycle is 13.12 kcal mol$^{-1}$ compared to an ideal value of 11.38 kcal mol$^{-1}$. We calculated the energies of $[\mathrm{PdBr_2([9]aneS_3)}]$ in this conformation as 9.89 kcal mol$^{-1}$ and then constructed the equivalent molecule with the conformations (a), (b) or (g) (in the last two the third sulfur is bent away from the metal). The energies of these were 8.53, 8.99 and 12.01 kcal mol$^{-1}$ respectively.

While this result does not show that the observed conformation (e) has the lowest energy, it is noticeable that the difference in energies between (a) and (e) in metal complexes is only 1.36 kcal mol$^{-1}$, significantly less than the difference between ligand conformations in the gas phase (*e.g.* 2.49 kcal mol$^{-1}$ *via* the UFF force field).

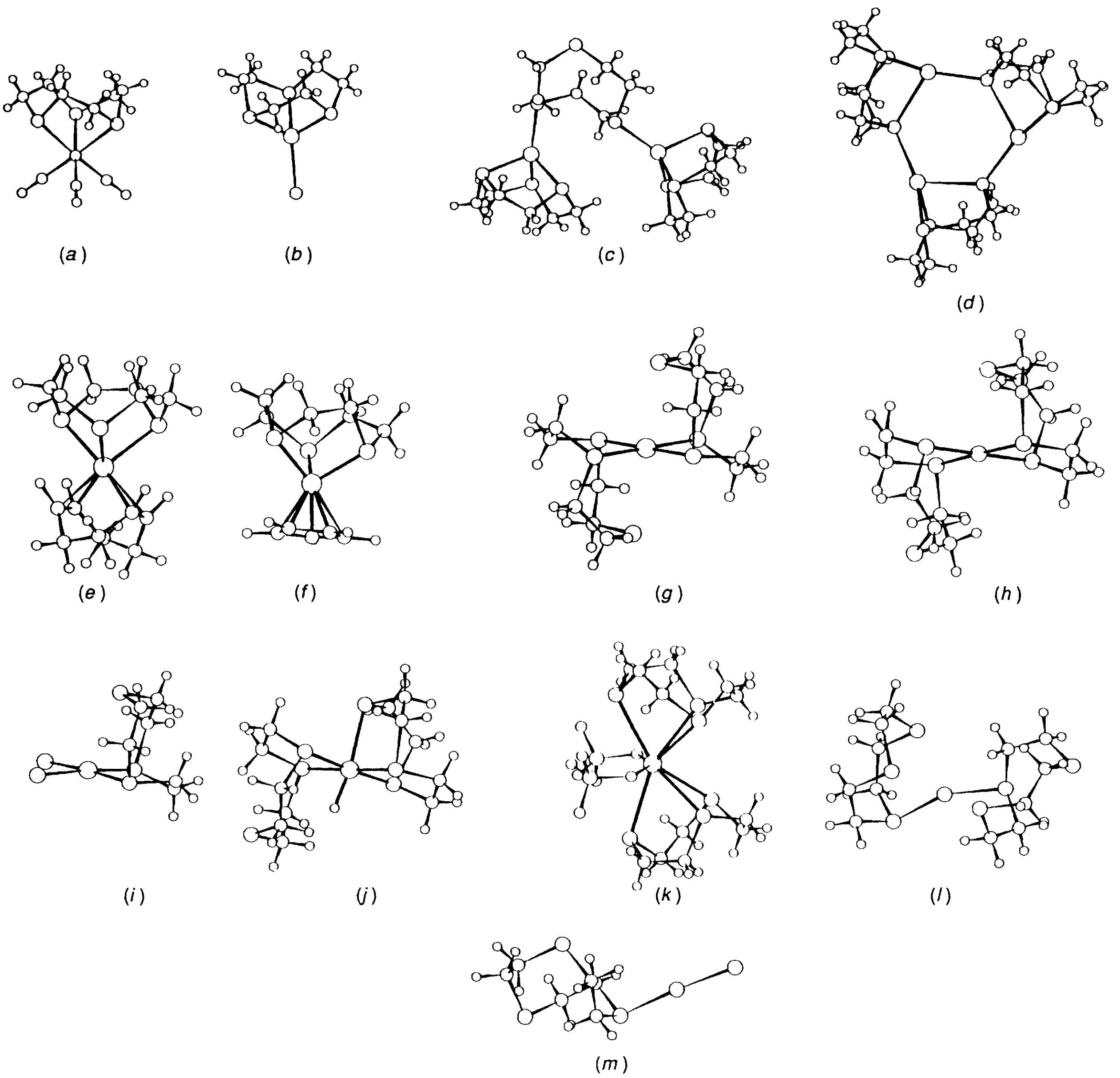

**Fig. 5** Various metal complexes of [9]aneS$_3$: (*a*) [Re(CO)$_3$([9]aneS$_3$)]$^+$ (GIFLAI), (*b*) [CuI([9]aneS$_3$)] (FITDUH), (*c*) [Cu$_2$([9]aneS$_3$)$_3$]$^{2+}$ (JAPXUT), (*d*) [Ag$_3$([9]aneS$_3$)$_3$]$^{3+}$ (FITDOB), (*e*) [Rh(cod)([9]aneS$_3$)]$^+$ (KILRIH), (*f*) [Fe($\eta$-C$_5$H$_5$)([9]aneS$_3$)]$^+$ (JAGNUA), (*g*) [Pd([9]aneS$_3$)$_2$]$^{2+}$ (FAPBED), (*h*) [Pt([9]aneS$_3$)$_2$]$^{2+}$ (FAGSAH), (*i*) [PdBr$_2$([9]aneS$_3$)] (FAPBIH), (*j*) [IrH([9]aneS$_3$)$_2$]$^{2+}$ (JEKRIA), (*k*) [Pb(ClO$_4$)$_2$([9]aneS$_3$)$_2$] (VEJNIH), (*l*) [Au([9]aneS$_3$)$_2$]$^+$ (KAMXOL), and (*m*) [AuCl([9]aneS$_3$)] (JAFLEH)

*Other complexes.* Table 7 details the remaining complexes which fall into none of the above categories. Modelling results are given in Table 8(*d*). In [IrH([9]aneS$_3$)$_2$]$^{2+}$ [Fig. 5(*j*)] one ligand has the usual conformation (a) while in the other only two sulfurs are bonded and the third is bent away from the metal, the octahedral co-ordination sphere around the iridium being completed by a Ir–H bond. The ligand conformation in this case is similar to that observed in (b) (all torsion angles are within 30°). We carried out minimisation of several possible structures of this complex but found the (a,b) conformation to have the lowest energy: 18.19 (a,b), 21.71 (a,a), 21.79 (a,e) and 20.12 kcal mol$^{-1}$ (a,g). It is surprising that conformation (a,a) has a relatively low energy despite the three sulfurs being in a facial environment. The third sulfur bends away from the metal to make room for the hydrogen atom. However not surprisingly the (a,b) conformation, where a sulfur atom is naturally bent away from the co-ordination sphere, has the lowest energy. The minimised structure fitted well with the experimental data.

The complex [Pb(ClO$_4$)$_2$([9]aneS$_3$)] [Fig. 5(*k*)] contains eight-co-ordinate lead bonded to six sulfur atoms and two monodentate perchlorate ions. This could not be modelled in the usual way with ideal angles because of the complexity of the geometry. We therefore used the MM2MX program[25] which allows for the incorporation of 1,3 interaction terms instead of angle-bending terms around metal centres. In previous work,[10] we have shown that this method is not superior to including angle-bending terms for metals with co-ordination numbers $\leqslant 6$. However for higher co-ordination numbers it is particularly useful.[26,27] In this particular case, the structure was reproduced well: bond lengths to within 0.02 Å and angles subtended at the metal to within 5°.

In both [Au([9]aneS$_3$)$_2$]$^+$ [Fig. 5(*l*)] and [AuCl([9]aneS$_3$)] [Fig. 5(*m*)] the gold atom is involved in only two short bonds in a distorted linear arrangement. In [Au([9]aneS$_3$)$_2$]$^+$ the metal is bonded to three sulfur atoms (one short at 2.25 and two long at 2.85 Å) of one macrocycle in conformation (g) and to one sulfur atom in the other with the (e) conformation. The (g,e) conformations of the two macrocycles differ from ideal values

(Table 2) by less than 25°. In [AuCl([9]ane$S_3$)] the gold is bonded to one sulfur atom of a macrocycle [in conformation (g)] and a chlorine atom. In this structure there are also some interactions with other molecules but at distances from the gold atom of over 3.0 Å. We found both molecules difficult to model primarily because of the low co-ordination number. We suspect that packing effects, as represented by the large number of weak interactions, play an important role particularly in the case of [AuCl([9]ane$S_3$)] which can be described as having a one-dimensional polymeric structure. It is interesting that in both these structures when only one sulfur atom of a macrocycle is bonded to a metal then that macrocycle adopts conformation (g) which unlike the other low-energy conformations allows the other two sulfur atoms to be directed away from the metal. This conformation is also found in $[Cu_2([9]aneS_3)_3]^{2+}$ where a macrocycle bridges between two metals. Similarly in $[Au([9]aneS_3)]^+$ we assess that conformation (e) is suitable for producing one short and two long bonds to a metal.

## Conclusion

We have successfully modelled the majority of the crystal structures containing the [9]ane$S_3$ macrocycle with a wide range of metals. It proved necessary to estimate carefully the ideal M–S bond length but otherwise a standard force field could be used. Many geometric distortions of the macrocycle in the differing environments were reproduced. Energy calculations indicated the lowest-energy conformations of a wide range of complexes and these fitted with experimental observations. We consider that it would be possible to predict the likely structure of the macrocycle with nearly all metals although perhaps the esoteric gold ion structures are unpredictable.

The universal force field[7] is an ambitious attempt at providing parameters for all elements. However it seems unlikely that it will be possible to generate ideal metal bond lengths for the complete variety of inorganic complexes based on metal radii, bond order and electronegativity alone. We have shown that to get the best fit to experimental data it is necessary carefully to parametrise for ideal bond lengths from known crystal structures of similar compounds before accurate predictions of structure can be made.

## Acknowledgements

We thank the Defence Research Agency (Fort Halstead, UK) for support.

## References

1 U. Burkert and N. L. Allinger, *ACS Monogr*, 1982, 177.
2 R. D. Hancock, *Acc. Chem. Res.*, 1990, **23**, 253.
3 G. R. Brubaker and D. W. Johnson, *Coord. Chem. Rev.*, 1984, **53**, 1.
4 K. R. Adam, M. Antolovich, L. G. Brigden and L. F. Lindoy, *J. Am. Chem. Soc.*, 1991, **113**, 3346.
5 T. N. Doman, C. R. Landis and B. Bosnich, *J. Am. Chem. Soc.*, 1992, **114**, 7264.
6 M. G. B. Drew and P. C. Yates, *Pure Appl. Chem.*, 1989, **61**, 835.
7 A. K. Rappe, C. J. Casewit, K. S. Colwell, W. A. Goddard III and W. M. Skiff, *J. Am. Chem. Soc.*, 1992, **114**, 10024.
8 M. G. B. Drew, S. Hollis and P. C. Yates, *J. Chem. Soc., Dalton Trans.*, 1985, 1829.
9 M. G. B. Drew and P. C. Yates, *J. Chem. Soc., Dalton Trans.*, 1987, 2563.
10 M. G. B. Drew and M. A. Santos, *Struct. Chem.*, 1993, **4**, 5.
11 S. R. Cooper and S. C. Rawle, *Struct. Bonding (Berlin)*, 1990, **72**, 1.
12 R. S. Glass, G. S. Wilson and W. N. Setzer, *J. Am. Chem. Soc.*, 1980, **102**, 1068.
13 R. Blom, D. W. H. Rankin, H. E. Robertson, M. Schroder and A. Taylor, *J. Chem. Soc., Perkin Trans.*, 1991, 2773.
14 M. Lipton and W. C. Still, *J. Comput. Chem.*, 1988, **9**, 343.
15 M. Saunders, K. N. Houk, Y-D. Wu, W. C. Still, M. Lipton, G. Chang and W. C. Guida, *J. Am. Chem. Soc.*, 1990, **112**, 1419.
16 J. M. Goodman and W. C. Still, *J. Comput. Chem.*, 1991, **12**, 1110.
17 H.-J. Bohm, G. Klebe, T. Lorenz, T. Mietzner and L. Siggel, *J. Comput. Chem.*, 1990, **11**, 1021.
18 D. M. Ferguson and D. J. Raber, *J. Am. Chem. Soc.*, 1989, **111**, 4371.
19 QUANTA/CHARMm, version 3.2, Molecular Simulations Inc., Waltham, MA, 1992.
20 W. A. Dollase, *Acta Crystallogr., Sect. A*, 1974, **30**, 513.
21 MATCH program, M. G. B. Drew and J. U. Smith, 1992, unpublished work; J. U. Smith, Ph.D. Thesis, University of Reading, 1992.
22 CERIUS, Version 3.0, Molecular Simulations Inc., Cambridge, 1992.
23 R. D. Hancock, S. M. Dobson and J. C. A. Boeyens, *Inorg. Chim. Acta*, 1987, **133**, 221.
24 Cambridge Crystallographic Database, 1992 update.
25 D. M. Ferguson and D. J. Raber, MM2MX, Q.C.P.E. Program No. 588, Quantum Chemistry Program Exchange, Indiana University, IN, 1990.
26 D. J. Brecknell, D. J. Raber and D. M. Ferguson, *J. Mol. Struct.*, 1985, **124**, 343
27 D. M. Ferguson and D. J. Raber, *J. Comput. Chem.*, 1990, **11**, 1061.

*Received* 11*th June* 1993; *Paper* 3/03376G